Carbon 100 (2016) 625–631

Contents lists available at ScienceDirect

Carbon

journal homepage: www.elsevier.com/locate/carbon

Influence of Au doping on electrical properties of CVD graphene

Aleksandra Krajewska [a, b], Krzysztof Oberda [a], Jon Azpeitia [c], Alejandro Gutierrez [d], Iwona Pasternak [a], Maria F. López [c], Zygmunt Mierczyk [b], Carmen Munuera [c], Wlodek Strupinski [a, *]

[a] Institute of Electronic Materials Technology, Wolczynska 133, 01-919 Warsaw, Poland
[b] Institute of Optoelectronics, Military University of Technology, Gen. S. Kaliskiego 2, 00-908 Warsaw, Poland
[c] Instituto de Ciencia de Materiales de Madrid, Consejo Superior de Investigaciones Científicas, Cantoblanco, ES-28049 Madrid, Spain
[d] Departamento de Física Aplicada, Instituto de Ciencia de Materiales Nicolás Cabrera, Universidad Autónoma de Madrid, Cantoblanco, E-28049 Madrid, Spain

ARTICLE INFO

Article history:
Received 11 October 2015
Received in revised form
5 January 2016
Accepted 17 January 2016
Available online 19 January 2016

ABSTRACT

In this study we report on the effective p-doping of chemical vapor deposition (CVD) graphene transferred from copper foil onto SiO_2/Si and PET substrates. Tetrachloroauric acid ($HAuCl_4$) is used to promote graphene doping with a direct correlation between its concentration and modification of graphene's electrical properties. The doping mechanism entails the charge transfer (CT) between Au^{III} ions and graphene, and the formation of Au nanoparticles (AuNPs) on the surface. X-ray photoelectron spectroscopy (XPS) was employed to confirm this charge transfer, whereas the presence of the AuNPs was verified based on Scanning Electron Microscopy (SEM) and Atomic Force Microscopy (AFM) images. The influence of doping on the electrical properties of graphene was assessed by Kelvin Probe Microscopy (KPM) and standard Hall Effect measurements, proving the ability of the method to effectively tune the carrier concentration, achieving sheet resistances as low as 79 Ω/sq. The controlled tuning of the electrical properties together with the use of flexible substrates makes the presented results a very interesting approach enabling the development of a variety of industrial applications, including flexible electronics.

1. Introduction

Graphene is characterised by a combination of unique electrical, thermal and optical properties [1–4] that together make it a promising candidate for applications that require the use of conductive, transparent and flexible material [5–8]. Such potential use of graphene as transparent conducting film relies mainly on two parameters, i.e. high transmittance and low sheet resistance. It is generally agreed that to replace one of standard commercial transparent electrodes (indium tin oxide, ITO) such materials must, at the very least, display a sheet resistance of $Rs < 100\ \Omega$/sq, coupled with transmittance of $T \approx 80–90\%$ in the visible [9]. Regarding the latter parameter, graphene fulfils the above requirements, with T close to 90% [9]. Yet, the values reported for sheet resistance in as-transferred graphene (up to now, a transfer process has been needed to place graphene on the device) are still below the acceptable level for industrial applications. Nonetheless, there is still much room for improvement, especially when considering the possibilities of post-transferred graphene modification. Among them, chemical doping is a promising approach to intentionally modulating graphene carrier transport properties and reaching a top quality material with the required specifications [10,11]. For a successful outcome after the doping process, controlling the charge carrier type and concentration is mandatory. The properties of chemically modified graphene depend on the type of the dopant used, in particular on its constituent elements and functional groups, and also on the nanostructuring of the dopant material [12]. N-type graphene is a result of graphene doping, among others with hydrazine and polyethyleneimine [13,14], titanium and potassium [15] atoms or NH_3 molecules [16], while p-type graphene can be obtained with NO_2 [17], F4-TCNQ [18], metal chlorides or gold complexes such as $AuCl_3$, $IrCl_3$, $MoCl_3$, $OsCl_3$, $Au(OH)_3$ and Au_2S [19–21]. In particular, $AuCl_3$ is a promising p-type dopant, allowing a facile control of the doping degree by changing the $AuCl_3$

* Corresponding author.
E-mail address: wlodek.strupinski@itme.edu.pl (W. Strupinski).

http://dx.doi.org/10.1016/j.carbon.2016.01.066
0008-6223/

concentration [22] or the doping time [23]. The reported changes in the sheet resistance and optical transmittance of $AuCl_3$-treated graphene [22] prove the suitability of this approach and show the possibility of finally meeting the challenges imposed on graphene applications by the industry. Tetrachloroauric acid ($HAuCl_4$) can be treated as a another suitable candidate for graphene p-doping based on its proved ability to easily dope C_{60} molecules with holes via spontaneous electron transfer from C_{60} to Au^{III} ions [24] and when following the said approach. Also, since $HAuCl_4$ is a common precursor in the synthesis of AuNPs and gold has a lower Fermi level (Eo vs. NHE = +1.002 V, corresponding to −5.5 eV) than graphene (4.4 eV) [25], the formation of nanoparticles on the graphene surface is viable option. This is related to the fact that electrons are supposed to be transferred from graphene to Au^{III} ions when graphene is in contact with the $HAuCl_4$ solution (CT mechanism). The Au^{III} ions coming from $HAuCl_4$ can be regarded as a p-type dopant. Furthermore, the use of $HAuCl_4$ is a straightforward method to synthesize graphene-AuNPs materials in an efficient one-step process. Using $HAuCl_4$ allows intentional control over the doping process due to the fact that the application of different $HAuCl_4$ concentrations is feasible.

In this study we investigate an effective p-doping with $HAuCl_4$ of both, monolayer and few-layer CVD-grown graphene, transferred onto two different substrates (SiO_2/Si and PET). Characterization of the doping process, based on the charge transfer from graphene to Au^{III} ions and the formation of AuNPs on graphene's surface, was performed by XPS, SEM and AFM. The effect of doping on the electrical properties of the system was studied as a function of $HAuCl_4$ concentration. The reported results demonstrate the potential of the method for tailoring the properties of graphene, yielding graphene with a very low sheet resistance and a high p-type carrier concentration.

2. Experimental

2.1. Graphene growth and transfer

Monolayer graphene was grown by Chemical Vapor Deposition (CVD) on 25 μm-thick copper foil (Alfa Aesar, 99.999% metals basis) using the commercially available Black Magic Pro system. Prior to growth, copper samples were pre-treated at 960 °C under Ar and H_2 gas mixture conditions followed by H_2 gas flow at the pressure of 20 mbar. The purpose of this step was to improve the quality and increase the grain size of Cu substrates as well as to remove oxides from the copper surface. Next, methane was introduced into the reactor and graphene layer started to cover the copper substrate. Finally, copper with graphene on top was cooled down to room temperature in Ar atmosphere.

After the growth process, graphene was transferred onto high-resistivity silicon (>1000 Ωcm) with a 300 nm layer of silicon oxide and polyethylene terephthalate substrates, using the high-speed electrochemical delamination method [26]. At first, copper foil with graphene on top was spin-coated with a thin layer of poly(methyl methacrylate) (PMMA) (4% in anisole) and cut into 1 × 1.5 cm small pieces. Then Cu/graphene/PMMA was placed in potassium chloride solution (KCl, 1 mol/dm^3) and detached during an electrochemical process. Graphene/PMMA was subsequently cleaned in deionized (DI) water, transferred onto the substrate and heated to 130 °C. PMMA was removed with acetone.

2.2. Doping with $HAuCl_4$

Tetrachloroauric acid (Avantors Performance Materials Poland S.A., 30% $HAuCl_4$, pure) of different concentrations (0.1%, 1%, 5%, 15% and 30%) was used to dope graphene on the SiO_2/Si substrate. $HAuCl_4$ with a concentration of 30% was also used to dope one, two, three and four graphene layers on the PET substrate. Each time 20 μl of the dopant solution was poured over graphene and spin-coated at 1500 rpm for 30 s.

2.3. Characterization

The electrical properties of graphene samples before and after doping were measured by the Hall method in van der Pauw geometry (0.55 T Ecopia HMS-3000 Hall Measurement System) in ambient atmosphere. The morphology of graphene was investigated using Scanning Electron Microscopy (SEM) (Auriga Cross-Beam Workstation (Carl Zeiss)). To show the size and size distributions of AuNPs the ultra-high resolution SEM equipment was used (Hitachi SU 8230, 30 kV, secondary electron image resolution of 0.8 nm). A commercial Atomic Force Microscopy (AFM) system with software from Nanotec [27] operating in ambient conditions was also employed to perform morphological and surface potential (KPM) characterizations. X-ray photoelectron spectroscopy (XPS) (CLAM4 electron energy analyser and a twin anode (Mg and Al) X-ray source from Thermo-Scientific) was performed to determine the chemical composition of the graphene layers, prior and after doping. For different samples, high resolution core level peaks of C-1s and Au-4f were measured. In order to accommodate the typical asymmetric line shape of sp^2 carbon, this component was fitted using a Doniach and Sunjic function and an asymmetry parameter of 0.068 [28]. For the Au-4f region, 4f doublets were used, with the appropriate spin–orbit splitting and ratio between $4f_{7/2}$ and $4f_{5/2}$ components.

3. Results and discussion

The doping effect of $HAuCl_4$ is based on the charge transfer between graphene and Au^{III} ions. In contact with graphene, Au^{III} ions are reduced to AuNPs, withdrawing electrons from the graphene, as shown schematically in Fig. 1. This would result in a p-type doping, the degree of which can be controlled by the $HAuCl_4$ concentration. Similar processes were described in literature, where the charge transfer process through reduction of Au^{III} to AuNPs was monitored by Raman and Localized Surface Plasmon Resonance (LSPR) spectroscopy [22,29]. The amount of charge that can be transferred from graphene without damaging its structure still remains an open question [21,24,30,31].

In order to assess the proposed transfer mechanism, XPS measurements were performed and the elemental composition of the components at graphene's surface was studied. High resolution core level peaks of C-1s and Au-4f were measured for different samples.

In Fig. 2a we can observe the C-1s XPS spectrum corresponding to an undoped sample. To properly fit the C-1s emission signal, four sub-spectra were needed. The main signal corresponds to the sp^2 hybrid of the C–C bond at a binding energy (BE) of 284.5 eV. The peaks located at BE of 285.4 and 286.2 eV can be assigned to functional groups on graphene such as C–OH and C–O, respectively. Finally, the signal at 289.1 eV BE corresponds to the O=C–O and C–C=O groups. In this figure we can observe the low intensity of the C–OH, C–O, O=C–O and C–C=O components, evidencing a high quality of the graphene layer. As shown in panel b, the spectra for graphene doped with dopant concentration of 15% shows a similar shape, exhibiting also the main C–C sp^2 component and low concentration of other carbonaceous species. The discrete changes of the C-1s core level spectrum prior to graphene doping (Fig. 2) and after graphene doping suggest a negligible character of the charge transfer (CT) between graphene and Au^{III} ions [32]. No relevant differences can be found between undoped and doped

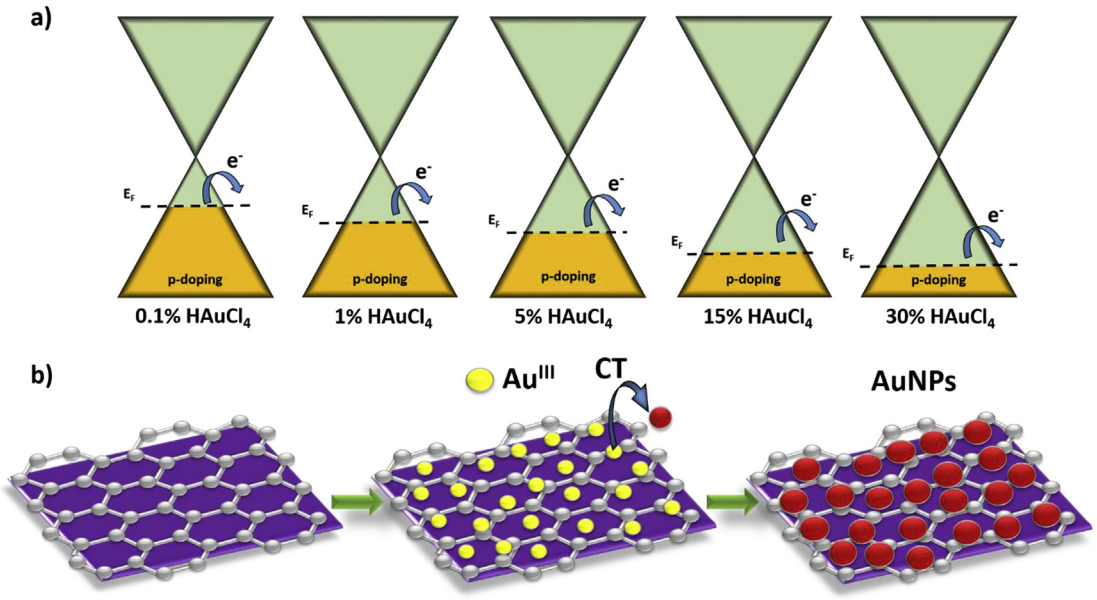

Fig. 1. Illustration of the induced Fermi level shifts with $HAuCl_4$ solution concentrations (a) and proposed reduction mechanism of Au^{III} ions to AuNPs after doping CVD graphene layers with $HAuCl_4$ solution (b) (A colour version of this figure can be viewed online).

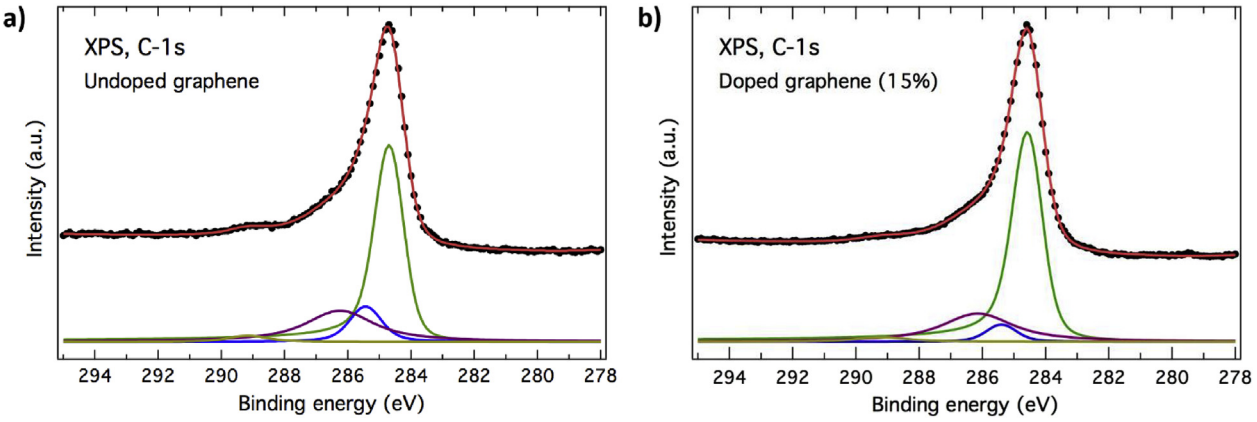

Fig. 2. High resolution XPS C-1s core level spectrum (black) prior to graphene doping (a) and after graphene doping (b) (A colour version of this figure can be viewed online).

graphene, which indicates that the doping process does not have any influence on the quality of the graphene layer.

To investigate the doping process, the Au-4f signal was analysed for different doping concentrations. The XPS spectrum of Fig. 3a shows the Au-4f signal after graphene doping with 30% concentration of $HAuCl_4$ solution. To fit the spectrum two doublets, corresponding to the $4f_{7/2}$ and $4f_{5/2}$ final states and separated by the Au-4f spin–orbit splitting, 4.2 eV, were needed. One of the doublets located at a BE of 83.5 eV corresponds to metallic gold and the second doublet at 85.6 eV is ascribed to Au^{III}. As can be observed, the fitted spectrum exhibits a predominant metallic gold signal, while the Au^{III} emission is less important. The XPS data indicate that the Au^{III} ions in contact with the graphene surface undergo reduction, which leads to a metallic state. These results evidence the existence of a reduction mechanism of the Au^{III} ions to form AuNPs on the graphene's surface.

Additionally, Fig. 3b presents the effect of the dopant concentration on the efficiency of the reduction process. As the dopant concentration is increased, an enhancement of the Au emission is observed, except for the sample doped with 30% $HAuCl_4$, which has a similar intensity to that doped with 15% $HAuCl_4$, which suggests that saturation occurs for high $HAuCl_4$ concentrations. In all cases, the behaviour of the XPS emission suggests the diffusion of the Au ions on the graphene layer, which favours its combination to form discrete AuNPs.

Morphological changes on graphene induced by the doping process were investigated by means of Scanning Electron Microscopy and Atomic Force Microscopy analysis. Fig. 4 presents SEM and AFM images of graphene on SiO_2/Si prior to (0%) and after doping with $HAuCl_4$ solution of different concentrations. For the undoped sample, the typical morphology of graphene on SiO_2/Si is observed, with wrinkles along the surface and darker patches (in the SEM images) that correspond to bilayer graphene. After spin-coating the $HAuCl_4$ solution on top of graphene, the overall morphology remains similar to the undoped sample. However, a closer look at the SEM images evidences the existence of small bright dots, whose number increases with increasing concentration. These correspond to the AuNPs formed during the doping process that decorate the entire surface. The histograms (Fig. 5) show the average size and size distributions of AuNPs after doping

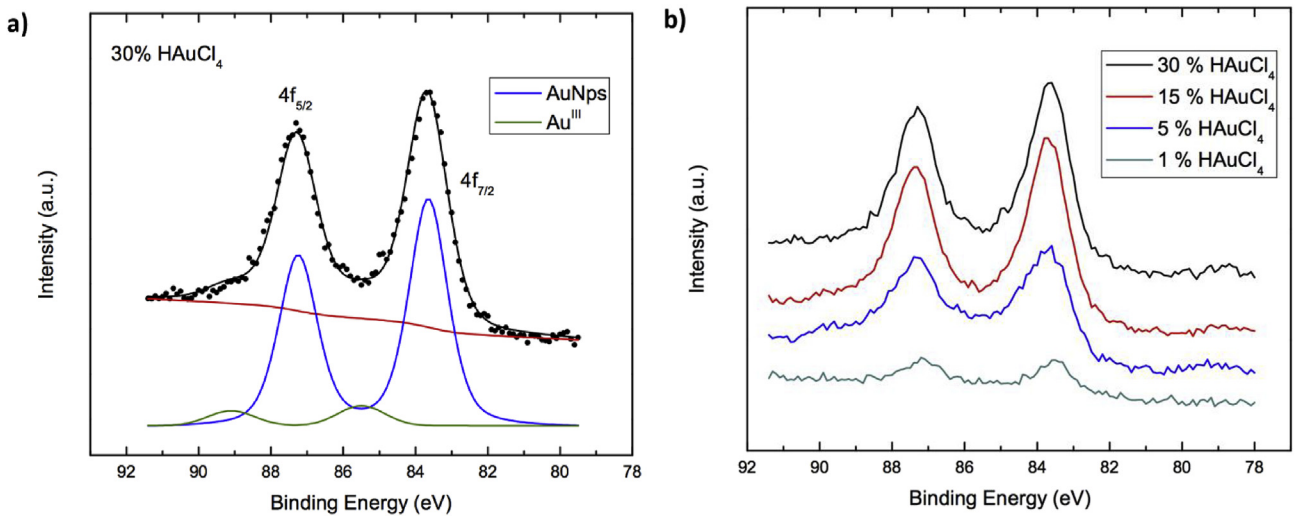

Fig. 3. Binding energy of Au^{III} and AuNPs 4f after graphene doping with 30% concentration of $HAuCl_4$ solution (a), XPS peaks intensity of Au-4f as a function of dopant concentration (b) (A colour version of this figure can be viewed online).

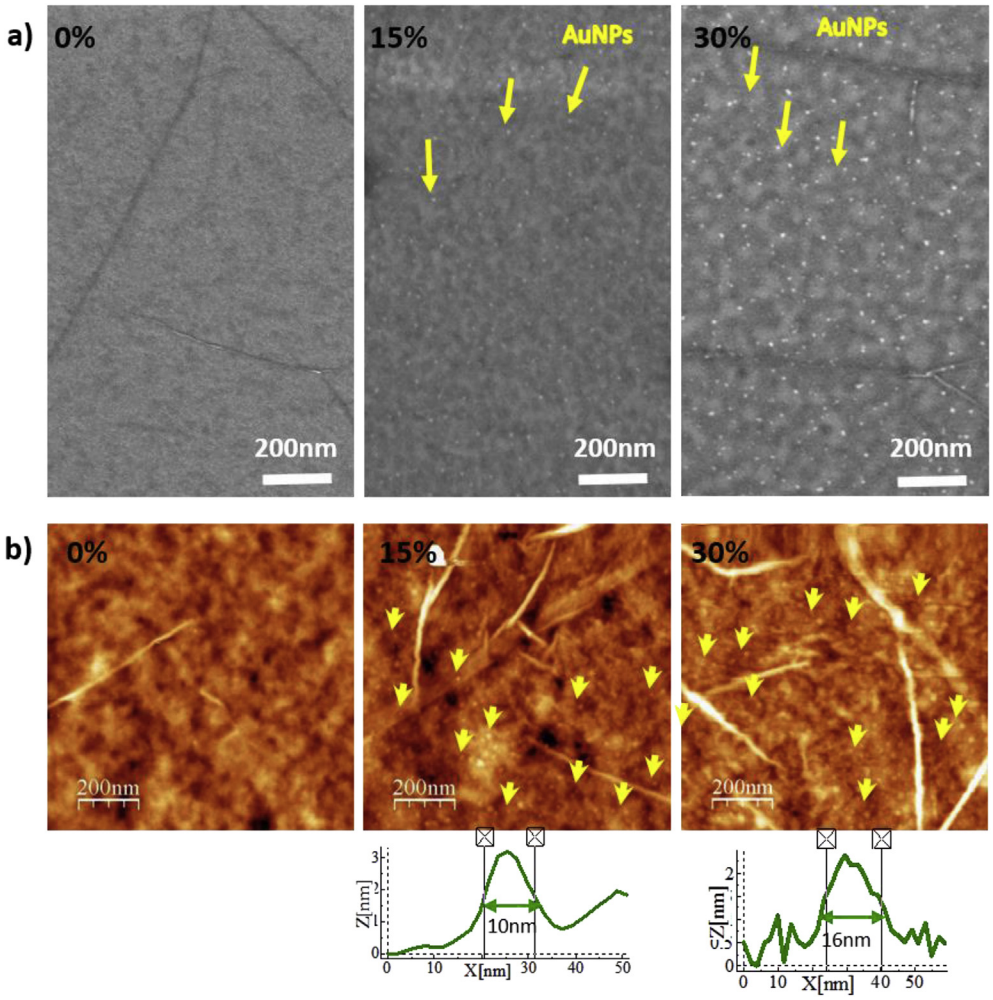

Fig. 4. SEM (a) and AFM (b) images of graphene layers on SiO_2/Si substrates without (0%) and with Au nanoparticles for different doping concentrations (A colour version of this figure can be viewed online).

with $HAuCl_4$ solution concentrations of 15% and 30%. The AuNPs diameter ranges between 8–12 nm and 4–8 nm for 30% and 15% $HAuCl_4$ solutions, respectively. AFM images of the doped samples also show the presence of rounded clusters all over the surface that

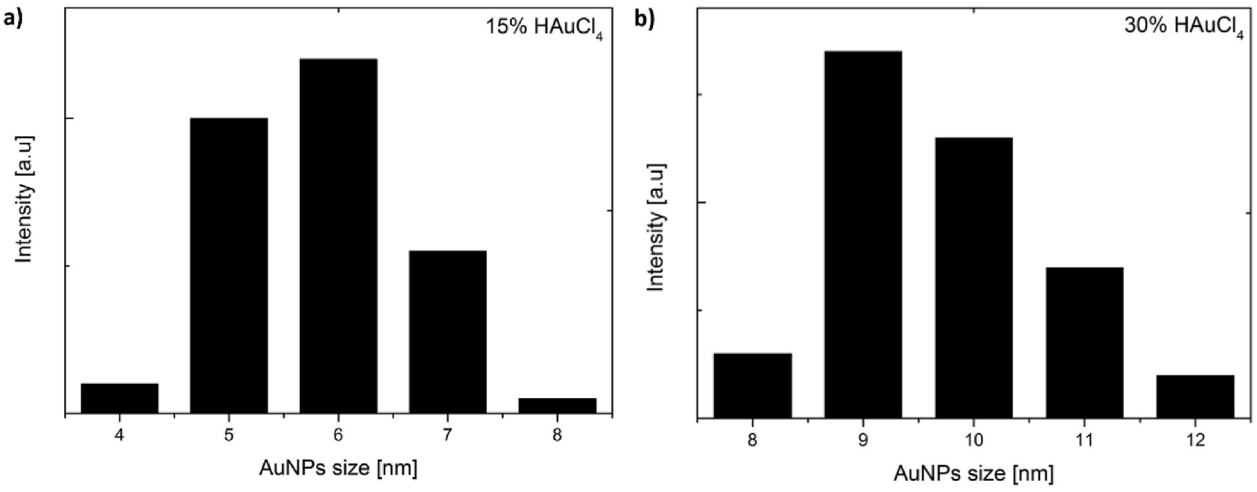

Fig. 5. Histograms of the average size and size distributions of AuNPs for graphene layers on SiO_2/Si substrates doped with $HAuCl_4$ solution concentrations of 15% (a) and 30% (b).

can be identified with the AuNPs. Line profiles taken along these clusters were used to measure the size of the AuNPs (Fig 4b). For 15% $HAuCl_4$ solution the average dimensions were 10 nm in diameter and 1–3 nm in height. For 30% $HAuCl_4$ solution, the average measured diameter was slightly larger, i.e. ~12–16 nm, but the height remained approximately the same, i.e. 2–3 nm. Taking into account the convolution effect of the AFM tips for features smaller than the tip radius, we can conclude that the measured diameter is overestimated due to this effect. So, considering the height as the correct measure, the spherical nanoparticles would have a diameter below 5 nm.

Since the AuNPs formation through charge transfer from graphene to the Au^{III} ions should not only alter the surface morphology but also the electrical properties, Kelvin Force Microscopy (KPM) was employed to investigate the surface potential (SP) variations for different dopant concentrations. This technique, which is a variant of AFM, is widely used in many areas of surface science because of its ability to nondestructively characterize the electrostatic properties of materials under ambient conditions [33]. In close relation with this work, KPM was successfully applied to investigate the doping character, doping ratio or work function changes in different graphene doped systems [12,23,34,35]. Fig. 6 collects the simultaneous topographic and surface potential (SP) images of the reference sample (undoped) as well as graphene samples with dopant concentration of 1%, 15% and 30%. To facilitate comparison between SP images, a plane offset was subtracted to all of them to keep the same colour scale for different samples.

For the reference sample, the SP image is relatively homogeneous, with a brighter contrast found in the wrinkle area (top right corner). After doping, the morphology retains its original shape for all used concentrations, as commented above. However, surface potential maps show measurable changes even for the lowest doping concentration. For the sample doped with 1% $HAuCl_4$, darker domains with sizes ranging between 100 and 200 nm are observed, with SP values ~120 mV lower than for the surrounding background. Additionally, the wrinkles that, on the undoped sample, show brighter SP contrast, in the case of the doped samples appear with lower contrast than the surrounding. AuNPs are unobservable even in topographic images when using 1% $HAuCl_4$ solution. Nonetheless, the darker spots in SP images can be ascribed to these AuNPs, responsible for the noticeable changes. The higher change at the wrinkles would agree with the higher concentration of AuNPs observed at those defects, as shown in the SEM image in Fig. 4. For the $HAuCl_4$ solution concentrations of 15% and 30% the SP image shows a more uniform signal. Darker spots are distinguishable in the surface potential map, and when correlated with the corresponding topography (colour circles), in most cases they can be associated with the presence of a cluster, thus indicating that the presence of AuNPs locally influences the electrostatic characteristics of the graphene sample. Besides these darker domains observed in the SP map of the doped samples, the average SP value (calculated from raw SP images, with no plane subtraction) also changes with dopant concentrations. The trend is plotted in Fig. 7 and shows a clear dependence on the $HAuCl_4$ concentration.

By definition, the measured surface potential (VSP) is related to the work function of the sample (φS) (equation (1)) [36].

$$eV_{SP} = \varphi T - \varphi S \quad (1)$$

where φT is the work function of the tip. Surface potential maps, therefore, measure changes in work function, which reflects both electrochemical (doping level) and electrostatic effects [37]. From (1), a lower V_{SP} indicates higher work function. Taken a constant value for the work function of the tip for all the measurements performed (this was checked routinely with a test sample of known φ), the decreasing trend in the V_{SP} as a function of the concentration is a clear evidence of the increase of p-doping with concentration [12,34,38].

The influence that $HAuCl_4$ doping has on the electrical properties of graphene was verified through Hall Effect measurements. Changes in graphene's sheet resistance (R), carrier concentration (n) and carrier mobility (μ), before and after doping, are collected in Table 1. The as-transferred graphene on SiO_2/Si had a sheet resistance ranging between 900 and 1100 Ω/sq and carrier mobility between 1000 and 1300 cm^2/V. The carrier concentration was always p-type and in the $(4–7) \times 10^{12}$ cm^{-2} range, which is typical for graphene transferred from copper [26]. After doping with $HAuCl_4$, the sheet resistance was reduced by about 30% when using 0.1% concentration of $HAuCl_4$ solution and even by 75% when using 30% concentration of $HAuCl_4$ solution. The carrier concentration increased up to 5.8×10^{13} cm^{-2} (30% $HAuCl_4$) and carrier mobility decreased to 409 cm^2/V (30% $HAuCl_4$). It was found that the higher concentration of $HAuCl_4$ solution, the more significant the rise in carrier concentration and reduction of sheet resistance.

Finally, CVD graphene with low sheet resistance on substrates like polyethylene terephthalate holds significant potential for future industrial applications including flexible graphene-based electronics and optoelectronics. In order to verify such

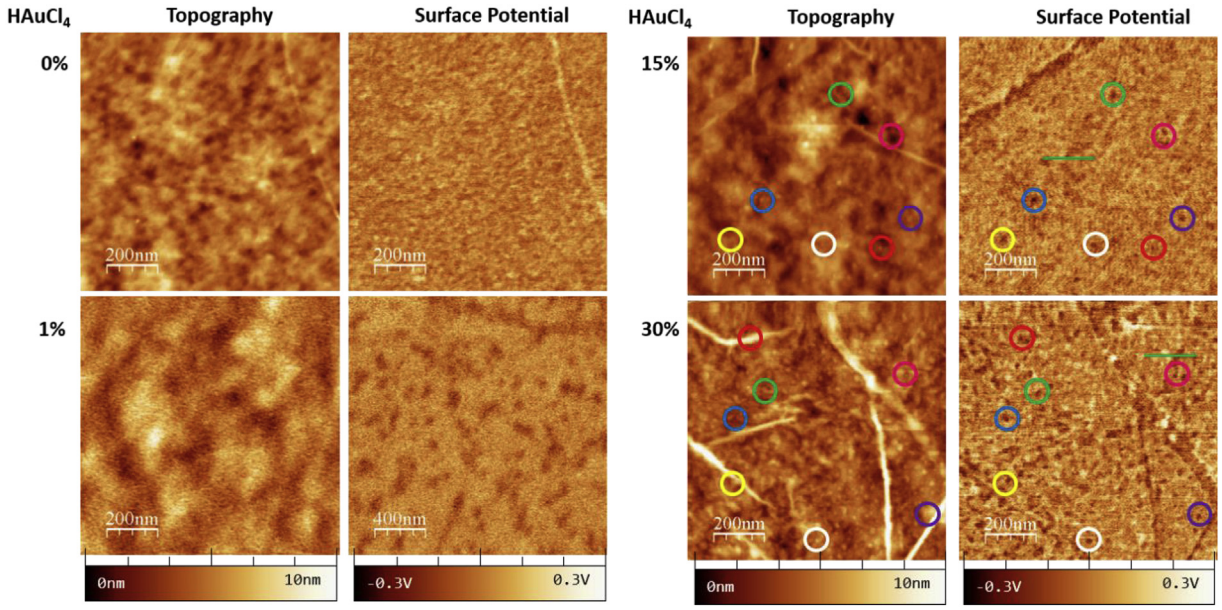

Fig. 6. Simultaneous topographic (left columns) and surface potential (right columns) images for graphene layers on SiO_2/Si substrates before and after doping with various $HAuCl_4$ solution concentrations (1%, 15% and 30%). 1 × 1 μm^2 scan area (A colour version of this figure can be viewed online).

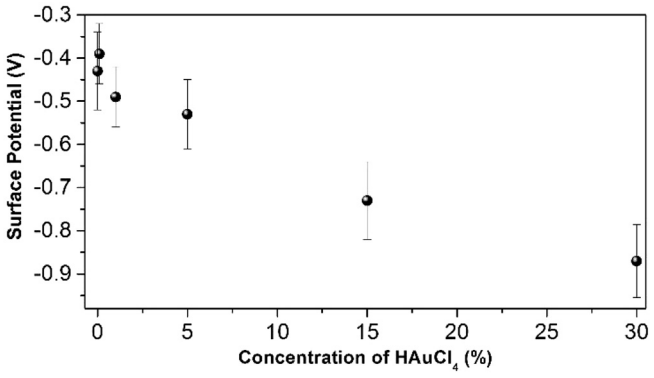

Fig. 7. SP value averaged for different images as a function of $HAuCl_4$ concentration.

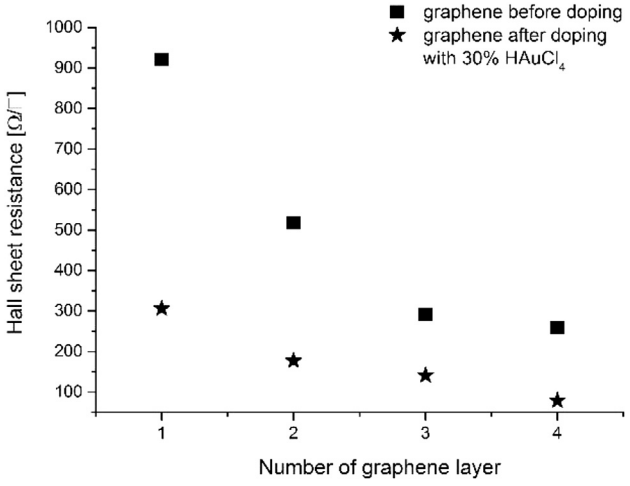

Fig. 8. Changes in the sheet resistance of graphene before and after doping with 30% concentration of $HAuCl_4$ solution as a function of the number of graphene layers.

applicability, one, two, three and four graphene layers were transferred onto a flexible and transparent PET substrate. The electrical parameters depend on the number of graphene layers. In four-layer graphene on the PET substrate the sheet resistance decreases down to ~250 Ω/sq, compared to ~1000 Ω/sq for monolayer graphene. Chemical doping using 30% concentration of $HAuCl_4$ solution decreases this value even further. In two-layer graphene, the sheet resistance decreases from 518 Ω/sq to 177 Ω/sq and from 259 Ω/sq to 79 Ω/sq for four-layer graphene upon solution doping. Fig. 8 presents the sheet resistance as a function of the number of graphene layers for graphene transferred to PET substrates.

4. Conclusions

In summary, CVD graphene grown on copper and transferred onto SiO_2/Si and PET substrates by high-speed electrochemical delamination was effectively p-doped with $HAuCl_4$. The higher concentrate of $HAuCl_4$ solution, the more effective the doping

Table 1
Electrical parameters of graphene before and after spin-coating different $HAuCl_4$ solution concentrations for graphene on SiO_2/Si substrates.

Before doping			Doping	After doping		
R [Ω/□]	n [cm^{-2}]	μ [cm^2/Vs]		R [Ω/□]	n [cm^{-2}]	μ [cm^2/Vs]
1181	+4,19E12	1261	0.1% $HAuCl_4$	869	+6,95E12	1032
976	+6,90E12	1032	1% $HAuCl_4$	661	+1,35E13	695
999	+5,35E12	1157	5% $HAuCl_4$	579	+1,40E13	766
963	+4,97E12	1303	15% $HAuCl_4$	401	+2,22E13	701
1180	+6,29E12	839	30% $HAuCl_4$	261	+5,85E13	409

process. It was shown that graphene's sheet resistance can be reduced even to 79 Ω/sq. XPS data show that the metallic gold signal predominates, thus evidencing the existence of a reduction mechanism of the Au^{III} ions to form AuNPs on the graphene's surface. The presence of this AuNPs formation was confirmed by SEM and AFM analysis. Our work indicates that doping with $HAuCl_4$ is a promising technology to produce p-doped graphene for many applications, including conductive, transparent and flexible materials.

Acknowledgements

The authors would like to thank Iwona Jozwik, PhD and Justyna Grzonka, PhD for the prepared SEM images. The research leading to these results has received funding from the European Union Seventh Framework Programme under grant agreement n°604391 Graphene Flagship. This work was also supported by the EU-FET grant GRAPHENICS 618086 and the Polish National Science Centre UMO-2013/09/N/ST5/02481.

References

[1] K.S. Novoselov, A.K. Geim, S.V. Morozov, D. Jiang, M.I. Katsnelson, I.V. Grigorieva, et al., Two-dimensional gas of massless dirac fermions in graphene, Nature 438 (2005) 197–200.
[2] Y. Zhu, S. Murali, W. Cai, X. Li, J.W. Suk, J.R. Potts, et al., Graphene and graphene oxide: synthesis, properties, and applications, Adv. Mater 22 (2010) 5226–5246.
[3] C. Lee, X. Wei, J.W. Kysar, J. Hone, Measurement of the elastic properties and intrinsic strength of monolayer graphene, Science 321 (2008) 385–388.
[4] M.J. Allen, V.C. Tung, R.B. Kaner, Honeycomb carbon: a review of graphene, Chem. Rev. 110 (1) (2010) 132–145.
[5] A.K. Geim, K.S. Novoselov, The rise of graphene, Nat. Mater 6 (2007) 183–191.
[6] A.K. Geim, Graphene: status and prospects, Science 324 (2009) 1530–1534.
[7] J.K. Wassei, R.B. Kaner, Graphene, a promising transparent conductor, Mater. Today 13 (2010) 52–59.
[8] R.R. Nair, P. Blake, A.N. Grigorenko, K.S. Novoselov, T.J. Booth, T. Stauber, et al., Fine structure constant defines visual transparency of graphene, Science 320 (2008) 1308.
[9] S. De, J.N. Coleman, Are there fundamental limitations on the sheet resistance and transmittance of thin graphene films? ACS Nano 4 (5) (2010) 2713–2720.
[10] T.O. Wehling, K.S. Novoselov, S.V. Morozov, E.E. Vdovin, M.I. Katsnelson, A.K. Geim, et al., Molecular doping of graphene, Nano Lett. 81 (2007) 173–177.
[11] H. Liu, Y. Liu, D. Zhu, Chemical doping of graphene, J. Mater. Chem. 21 (2011) 3335–3345.
[12] M.M. Giangregorio, W. Jiao, G.V. Bianco, P. Capezzuto, A.S. Brown, G. Bruno, et al., Insights into the effects of metal nanostructuring and oxidation on the work function and charge transfer of metal/graphene hybrids, Nanoscale 7 (2015) 12868–12877.
[13] J.B. Bult, R. Crisp, C.L. Perkins, J.L. Blackburn, Role of dopants in long-range charge carrier transport for p-type and n-type graphene transparent conducting thin films, ACS Nano 7 (8) (2013) 7251–7261.
[14] K.S. Mistry, B.A. Larsen, J.D. Bergeson, T.M. Barnes, G. Teeter, C. Enqtrakul, et al., n-Type transparent conducting films of small molecule and polymer amine doped single-walled carbon nanotubes, ACS Nano 5 (2011) 3714–3723.
[15] J.-H. Chen, C. Jang, S. Adam, M.S. Fuhrer, E.D. Williams, M. Ishigami, Charged-impurity scattering in graphene, Nat. Phys. 4 (2008) 377–381.
[16] X. Wang, X. Li, L. Zhang, Y. Yoon, P. Weber, H. Wang, et al., N-doping of graphene through electrothermal reactions with ammonia, Science 324 (2009) 768–771.
[17] S.Y. Zhou, D.A. Siegel, A.V. Fedorov, A. Lanzara, Metal to insulator transition in epitaxial graphene induced by molecular doping, Phys. Rev. Lett. 101 (2008) 086402.
[18] H. Pinto, R. Jones, J.P. Goss, P.R. Briddon, p-type doping of graphene with F4-TCNQ, J. Phys. Condens. Matter 21 (2009) 402001.
[19] K.C. Kwon, B.J. Kim, J.-L. Lee, S.Y. Kim, Role of ionic chlorine in the thermal degradation of metal chloride-doped graphene sheets, J. Mater. Chem. C 1 (2013) 253–259.
[20] K.C. Kwon, B.J. Kim, J.-L. Lee, S.Y. Kim, Effect of anions in Au complexes on doping and degradation of graphene, J. Mater. Chem. C 1 (2013) 2463–2469.
[21] F. Gunes,, H.-J. Shin, C. Biswas, G.H. Han, E.S. Kim, S.J. Chae, et al., Layer-by-layer doping of few-layer graphene film, ACS Nano 4 (2010) 4595–4600.
[22] K.K. Kim, A. Reina, Y. Shi, H. Park, L.J. Li, Y.H. Lee, et al., Enhancing the conductivity of transparent graphene films via doping, Nanotechnology 21 (28) (2010) 285205.
[23] Y. Shi, K.K. Kim, A. Reina, M. Hofmann, L.-J. Li, J. Kong, Work function engineering of graphene electrode via chemical doping, ACS Nano 4 (2010) 2689–2694.
[24] H.S. Shin, H. Lim, H.J. Song, H.-J. Shin, S.-M. Park, H.C. Choi, Spontaneous electron transfer from C60 to Au ions: oxidation of C60 and hole doping, J. Mater. Chem. 20 (2010) 7183–7188.
[25] A.M. Zaniewski, C.J. Trimble, R.J. Nemanich, Modifying the chemistry of graphene with substrate selection: A study of gold nanoparticle formation, Appl. Phys. Lett. 106 (2015) 123104.
[26] T. Ciuk, I. Pasternak, A. Krajewska, J. Sobieski, P. Caban, J. Szmidt, et al., Properties of chemical vapor deposition graphene transferred by high-speed electrochemical delamination, J. Phys. Chem. C 117 (2013) 20833–20837.
[27] I. Horcas, R. Fernández, J.M. Gómez-Rodríguez, J. Colchero, J. Gómez-Herrero, A.M. Baro, WSXM: A software for scanning probe microscopy and a tool for nanotechnology, Rev. Sci. Instrum. 78 (2007) 013705.
[28] J. Avila, I. Razado, S. Lorcy, R. Fleurier, E. Pichonat, D. Vignaud, et al., Exploring electronic structure of one-atom thick polycrystalline graphene films: A nano angle resolved photoemission study, Sci. Rep. 3 (2013) 2439.
[29] S. Lee, M.H. Lee, H.-J. Shin, D. Choi, Control of density and LSPR of Au nanoparticles on graphene, Nanotechnology 24 (2013) 275702.
[30] H.-J. Shin, W.M. Choi, D. Choi, G.H. Han, S.-M. Yoon, H.-K. Park, et al., Control of electronic structure of graphene by various dopants and their effects on a nanogenerator, J. Am. Chem. Soc. 132 (44) (2010) 15603–15609.
[31] D.W. Jeong, S. Park, W.J. Choi, G. Bae, Y.J. Chung, C.-S. Yang, et al., Electron-transfer transparency of graphene: Fast reduction of metal ions on graphene-covered donor surfaces, Phys. Status Solidi 9 (2015) 180–186.
[32] F. Joucken, Y. Tison, P. Le Fèvre, A. Tejeda, A. Taleb-Ibrahimi, E. Conrad, et al., Charge transfer and electronic doping in nitrogen-doped graphene, Sci. Rep. 5 (2015) 14564.
[33] C. Barth, A.S. Foster, C.R. Henry, A.L. Shluger, Recent trends in surface characterization and chemistry with high-resolution scanning force methods, Adv. Mater 23 (2011) 477–501.
[34] X. Wang, J.-B. Xu, W. Xie, J. Du, Quantitative analysis of graphene doping by organic molecular charge transfer, J. Phys. Chem. C 115 (15) (2011) 7596–7602.
[35] X. Zhou, S. He, K.A. Brown, J. Mendez-Arroyo, F. Boey, C.A. Mirkin, Locally altering the electronic properties of graphene by nanoscopically doping it with rhodamine 6G, Nano Lett. 13 (2013) 1616–1621.
[36] M. Nonnenmacher, M.P. O'Boyle, H.K. Wickramasinghe, Kelvin probe force microscopy, Appl. Phys. Lett. 58 (1991) 2921–2923.
[37] D.J. Ellison, B. Lee, V. Podzorov, C.D. Frisbie, Surface potential mapping of SAM-functionalized organic semiconductors by Kelvin Probe Force Microscopy, Adv. Mater 23 (2011) 502–507D.
[38] D. Ziegler, P. Gava, J. Güttinger, F. Molitor, L. Wirtz, M. Lazzeri, et al., Variations in the work function of doped single- and few-layer graphene assessed by Kelvin probe force microscopy and density functional theory, Phys. Rev. B 83 (2011) 235434.